



Technological University Dublin
ARROW@TU Dublin

Articles

School of Biological Sciences

2004-01-01


Molecular cloning and characterization of two mouse peroxisome proliferator-activated receptor alpha (PPARα) regulated peroxisomal acyl-CoA thioesterases.

Maria Westin
Karolinska Institute

Mary Hunt
Technological University Dublin, mary.hunt@tudublin.ie

Stefan Alexson
Karolinska Institute

Follow this and additional works at: <https://arrow.tudublin.ie/scschbioart>

 Part of the [Biochemistry Commons](#), and the [Molecular Biology Commons](#)

Recommended Citation

Westin M. A., Alexson S. E. H. and Hunt M. C. Molecular cloning and characterization of two mouse peroxisome proliferator-activated receptor alpha (PPARα) regulated peroxisomal acyl-CoA thioesterases. *J. Biol. Chem.* (2004) 279 (21): 21,841-21,848. doi:10.1074/jbc.M313863200

This Article is brought to you for free and open access by the School of Biological Sciences at ARROW@TU Dublin. It has been accepted for inclusion in Articles by an authorized administrator of ARROW@TU Dublin. For more information, please contact yvonne.desmond@tudublin.ie, arrow.admin@tudublin.ie, brian.widdis@tudublin.ie.



This work is licensed under a [Creative Commons Attribution-Noncommercial-Share Alike 3.0 License](#)



**Molecular cloning and characterization of two mouse
peroxisome proliferator-activated receptor alpha (PPAR α)
regulated peroxisomal acyl-CoA thioesterases.**

Maria A. K. Westin, Stefan E. H. Alexson and Mary C. Hunt

Department of Laboratory Medicine, Karolinska Institutet, Division of Clinical Chemistry, C1-74, Karolinska University Hospital at Huddinge, SE-141 86 Stockholm, Sweden.

Running title: Molecular characterization of peroxisomal acyl-CoA thioesterases

Key words: acyl-CoA thioesterase, acyl-CoA hydrolase, peroxisomes, lipid metabolism, acyl-CoA, α -oxidation.

Address for correspondence:

Dr. Mary C. Hunt
Department of Laboratory Medicine
Division of Clinical Chemistry C1-74
Karolinska Institutet
Karolinska University Hospital at Huddinge
SE-141 86 Stockholm
Sweden

Phone: +46-8-58581293
Fax: +46-8-58581260
email: mary.hunt@labmed.ki.se

ABSTRACT

Peroxisomes are organelles that function in the β -oxidation of very-long and long-chain acyl-CoAs, bile acid-CoA intermediates, prostaglandins, leukotrienes, thromboxanes, dicarboxylic fatty acids, pristanic acid and xenobiotic carboxylic acids. The very long- and long-chain acyl-CoAs are mainly chain-shortened and then transported to mitochondria for further metabolism. We have now identified and characterized two peroxisomal acyl-CoA thioesterases, named PTE-Ia and PTE-Ic, which hydrolyze acyl-CoAs to the free fatty acid and coenzyme A. PTE-Ia and PTE-Ic show 82% sequence identity at amino acid level and a putative peroxisomal type 1 targeting signal of -AKL was identified at the carboxy-terminal end of both proteins. Localization experiments using green fluorescent fusion protein showed PTE-Ia and PTE-Ic to be localized in peroxisomes. Despite their high level of sequence identity, we show that PTE-Ia is mainly active on long-chain acyl-CoAs, while PTE-Ic is mainly active on medium-chain acyl-CoAs. Lack of regulation of enzyme activity by free CoASH suggests that PTE-Ia and PTE-Ic regulate intra-peroxisomal levels of acyl-CoA, and they may have a function in termination of β -oxidation of fatty acids of different chain-lengths. Tissue expression studies revealed that PTE-Ia is highly expressed in kidney, while PTE-Ic is most highly expressed in spleen, brain, testis and proximal and distal intestine. Both PTE-Ia and PTE-Ic were highly upregulated in mouse liver by treatment with the peroxisome proliferator WY-14,643 and by fasting, in a peroxisome proliferator-activated receptor alpha (PPAR α) dependent manner. These data show that PTE-Ia and PTE-Ic have different functions based on different substrate specificities and tissue expression.

Abbreviations: PTE-Ia, peroxisomal acyl-CoA thioesterase Ia; PTE-Ic, peroxisomal acyl-CoA thioesterase Ic; CoASH, coenzyme A; PPAR α , peroxisome proliferator-activated receptor alpha; BSA, bovine serum albumin; PTE-2, peroxisomal acyl-CoA thioesterase 2; GFP, green fluorescent protein; PTS1, peroxisomal type-1 targeting signal; ORF, open reading frame.

INTRODUCTION

Peroxisomes are organelles present in most eukaryotic cells and play a key role in the metabolism of a variety of lipids such as very long-chain fatty acids, dicarboxylic fatty acids, bile acids, prostaglandins, leukotrienes, thromboxanes, pristanic acid and xenobiotic fatty acids, and in the biosynthesis of ether-linked glycerolipids such as plasmalogens and structural ether lipids abundant in the central nervous system (for reviews, see (1,2)). Peroxisomal α -oxidation of very long- and long-chain CoA esters results in chain-shortening of fatty acids which may then be transported to the mitochondria as carnitine esters for further oxidation. α -Oxidation of other types of lipids such as prostanoids leads to chain-shortening in the peroxisome for excretion as free carboxylic acids in the urine (3). Almost 30 years ago a group of compounds were identified which were shown to cause peroxisome proliferation in rodents, hence they were named peroxisome proliferators. Peroxisome proliferators are a structurally diverse group of compounds including plasticizers, hypolipidemic drugs (for example clofibrate), and WY-14,643. Peroxisome proliferators induce the expression of several genes involved in degradation of fatty acids, and cause peroxisome proliferation, hepatomegaly and hepatocarcinogenesis in rodent liver (4). These effects are mediated via the peroxisome proliferator-activated receptor alpha (PPAR α), which was shown to be a nuclear receptor in control of lipid metabolism (5,6). PPAR α induces the expression of many genes involved in peroxisomal and mitochondrial α -oxidation and β -oxidation of fatty acids, and targeted disruption of this receptor in mouse has established its key role as a mediator of lipid metabolism (6). Free fatty acids were identified as physiological, endogenous ligands for the PPAR α (7-10), which probably mediates the effects of PPAR α during fasting (11-14).

One group of enzymes which were previously identified to be responsive to treatment by peroxisome proliferators were the acyl-CoA thioesterases (for review see (15)). These enzymes are found in various compartments in the cell including cytosol, mitochondria, microsomes and peroxisomes. Acyl-CoA thioesterases catalyze the hydrolysis of acyl-CoAs to the free fatty acid and coenzyme A, thereby regulating intracellular content of various acyl-CoAs,

free fatty acids and free CoASH. The acyl-CoA thioesterase activity in peroxisomes was characterized and activity was identified with acyl-CoA esters from C₂- to C₂₀-CoA, with highest activity detected for medium- and long-chain acyl-CoAs (16). Since then, several peroxisomal acyl-CoA thioesterases have been cloned and characterized. A family of acyl-CoA thioesterases was identified in mouse, named Type-I acyl-CoA thioesterases, which at the time was shown to contain four highly homologous genes, two peroxisomal (PTE-Ia and -Ib), one mitochondrial (MTE-I), and one cytosolic (CTE-I), all of which are located in a cluster on mouse chromosome 12 (17). In human, four Type-I acyl-CoA thioesterases have been identified, with putative localizations in cytosol, mitochondria and peroxisomes (17,18). Another peroxisomal acyl-CoA thioesterase called PTE-2, which is unrelated to the Type-I gene family above, was identified as the major acyl-CoA thioesterase in mouse liver peroxisomes (19), with homologues in human, yeast and plants (20-23). This is a broad range acyl-CoA thioesterase that hydrolyzes almost all acyl-CoAs present in peroxisomes, including bile acid-CoA esters, short-, medium- and long-chain acyl-CoAs and intermediates from α -oxidation of pristanoyl-CoA. It is hypothesized that this enzyme is important in regulating intracellular levels of acyl-CoAs and CoASH during times of high α -oxidation and fatty acid overload.

In this study, we have cloned and characterized PTE-Ia and PTE-Ic, the latter which is a newly identified member of the Type-I family of acyl-CoA thioesterases. Both these enzymes are peroxisomal, are highly homologous (>80% sequence identity at amino acid level), and hydrolyze long-chain and medium-chain acyl-CoAs respectively. These enzymes may play a role in controlling acyl-CoA levels within the peroxisome in different tissues.

EXPERIMENTAL PROCEDURES

Chemicals- All commercially available acyl-CoAs used in this study were from Sigma (St. Louis, MO). Behenoyl-CoA, lignoceryl-CoA, cerotoyl-CoA and dimethylnonanoyl-CoA were kind gifts from Dr. Ronald Wanders.

Animals and treatments- All tissues used in this study were excised from adult male wild-type and PPAR α -null mice on a pure Sv/129 genetic background

(kindly provided by Dr. Frank Gonzalez and Dr. Jeffrey Peters). The mice were fed a standard chow diet (R36, Lactamin, Vadstena, Sweden) or alternatively fed a diet containing 0.1% WY-14,643 (Calbiochem-Novabiochem International) or fasted for 24 hours. Animals were sacrificed by CO₂ asphyxiation followed by cervical dislocation and tissues were excised and stored at -70°C for preparation of total RNA.

cDNA Cloning and Expression- The putative open reading frames for PTE-Ia (17) and PTE-Ic were derived from genomic databases and expressed sequence tags (ESTs) from the mouse EST database (www.ncbi.nlm.nih.gov), respectively, and were amplified using the following primers: for PTE-Ia: 5'-**C A T A T G** ATGTTTTCTGTATAATCACTCC-3' and 5'-**CATATGCACGCATTACCAC**-3' (which amplifies a splice variant named PTE-Ia 5':1 - see below), and for PTE-Ic using: 5'-**C A T A T G** TGTCACTACTCAAAGAAAATCAT-3' and 5'-**CATATGGTGCCAACAGTAAGCCT**-3' (Cybergene AB, Huddinge, Sweden), with the addition of an *Nde I* site (indicated in bold). The full-length open reading frames were amplified by reversed transcriptase-PCR (RT-PCR) using a template of WY-treated mouse liver total RNA. RT-PCR was performed using the One Step RNA PCR Kit (avian myeloblastosis virus (AMV)) (Takara Biomedicals). Thermal cycling for PTE-Ia was performed for 40 cycles at 94°C for 30 sec, 59°C for 30 sec, and 72°C for 2.5 min, followed by 72°C for 10 min. For PTE-Ic an annealing temperature of 55°C, 4 min extension and 35 cycles was used. The open reading frames were cloned into the *Nde I* site of the pET-16b plasmid (Novagen Inc.) and fully sequenced. For expression of PTE-Ia and PTE-Ic in BL21(DE3)pLysS cells, bacteria were cultured in 1 liter of Luria-Bertani medium at 37°C until an A_{600 nm} of about 0.6 was reached. Induction of protein expression for PTE-Ia was performed by addition of 1 mM isopropyl-1-thio-β-D-galactopyranoside (IPTG), and growth was continued for 3 h. PTE-Ic was induced with 0.2 mM IPTG and growth was continued for 15 h at 18°C. The bacteria were collected and frozen at -20°C. Bacterial pellets for PTE-Ia and PTE-Ic were thawed and resuspended in BugBuster[®] Protein Extraction Reagent (Novagen Inc.) with addition of Benzonase (Novagen Inc.), incubated for 20 min at room temperature and centrifuged at 16,000 × g for 20 min at 4°C. The supernatants were then used

for purification on a Hi-Trap[®] column (Amersham Biosciences, Inc.). Following equilibration of the column, the supernatant was applied, and the column was washed stepwise with 50, 100, 200, and 300 mM imidazole in 20 mM phosphate, 0.1 M sodium chloride to remove contaminating proteins. The PTE-Ia protein was eluted in the 500 mM imidazole fraction and PTE-Ic in the 300 mM imidazole fraction. These fractions were subsequently used for acyl-CoA thioesterase activity measurements.

Determination of Acyl-CoA Thioesterase Activity- Acyl-CoA thioesterase activity was measured spectrophotometrically at 412 nm with 5,5'-dithiobis (2-nitrobenzoic acid) (DTNB) (19). Since PTE-Ia thioesterase activity was inhibited at substrate concentrations higher than 5-10 μ M with acyl-CoAs between C₁₄-C₂₀, bovine serum albumin (BSA) was added at a molar ratio of BSA/acyl-CoA of 1:4.5. Enzyme activities were measured in three different recombinant protein preparations of PTE-Ia and in two recombinant protein preparations of PTE-Ic. The protein concentration was determined using the Bradford assay (24). The effect of CoASH on the enzyme activity was measured at 232 nm in phosphate buffered saline. The enzyme kinetics were calculated using Sigma Plot enzyme kinetics program.

Expression of PTE-Ia 5'-splice Variants: Since analysis of mouse expressed sequence tags (ESTs) indicated the existence of two different 5'-splice variants for PTE-Ia, these were examined in liver and kidney under normal conditions and during fasting using RT-PCR. The two splice variants were amplified using the following primers: PTE-Ia 5':1 5'-GACTTTTGTAGCGGTATCTT-3' (located at position 539-559 of cDNA sequence for 5':1 submitted to Genbank) and PTE-Ia 5':2 - 5' TTAGCTCTTGACCTTGTCTGTCTGC-3' (located at position 11-35 of cDNA sequence for 5':2 submitted to Genbank), together with a common primer 5'-CAGGTGGATAATGTCCATGTCCTTA-3' (located at position 1383-1407 of cDNA for 5':1 and 640-664 of cDNA for 5':2). The 5':1 splice variant was amplified by RT-PCR using an annealing temperature of 53°C for 1 min and 35 cycles, while for the 5':2 splice variant, 57°C for 35 cycles was used.

Localization of PTE-Ia and PTE-Ic using Green Fluorescent Fusion Protein and Cell Transfection Experiments- Oligonucleotides were designed based on the sequence of the open reading frames of PTE-Ia (5':1) and PTE-Ic for cloning as a fusion proteins with green fluorescent protein (GFP), to examine targeting of the proteins. The open reading frame of PTE-Ia (5':1) and PTE-Ic were amplified by RT-PCR, using the same primers used for cloning into the pET16b plasmid. Both PCR products were cloned into the pcDNA3.1/NT-GFP vector (Invitrogen) in frame with the GFP at the amino-terminal end. Sequence analysis was performed on the cloned products. In addition, two carboxy-terminal GFP constructs, one full-length construct, and one construct lacking the first 11 amino acids of PTE-Ia were cloned. These constructs were amplified using the following primers 5'-AGGATGCACGCATTTACCAC-3' (5':1), 5'-AGGATGGCACCTACTGTGAT-3' (5':2) and 5'-GTTTTGCTGGGATTGTCT-3' (common primer) and cloned into the pcDNA3.1/CT-GFP vector (Invitrogen) as described above.

Human skin fibroblasts from a control subject and a Zellweger patient were grown as described previously (19). Both control and Zellweger cells were grown overnight in 60-mm dishes on glass coverslips and were transfected with 10 μ g of PTE-Ia/GFP or PTE-Ic/GFP plasmid using the calcium phosphate method. Transfected cells were grown for 48 h and cells were fixed and prepared for immunofluorescence microscopy as described in (19). The cells were examined in Leica DM IRBE fluorescence microscope, using Hamamatsu C4742-95 Twain interface software.

Tissue Expression and Regulation by WY-14,643 and Fasting by RT-PCR- The tissue expression of PTE-Ia and PTE-Ic was examined in liver, kidney, heart, lung, adrenal, spleen, testis, muscle, brain, brown adipose tissue, white adipose tissue, proximal intestine, distal intestine, and gallbladder. The regulation by WY-14,643 was investigated in WY-treated livers from wild-type (+/+) and PPAR α -null (-/-) mice. Regulation by fasting was examined in liver, kidney and heart from wild-type and PPAR α -null mice. PTE-Ia was amplified using the following primers: 5'- TGGATGGCAAAAAGAAGACA-3' and 5'-GGGTGCCCAAGGAGGTCA-3' (representing a fragment of 505 bp from 2021-2525 of the 5':1 cDNA sequence submitted to Genbank, which will

amplify both variants 5':1 and 5':2 of PTE-Ia), and PTE-Ic using 5'-T A A T C A A T G G C G C C A C G G T C A A - 3' and 5'-CCAGCTATGTCACTACTCAAAGAA-3' (representing a 534 bp fragment from 900 – 1434 of the cDNA sequence). RT-PCR for PTE-Ia was performed for 35 cycles of 94°C for 30 sec, 48°C for 30 sec, and 72°C for 3 min, followed by 72°C for 10 min. For PTE-Ic, an annealing temperature of 54°C and extension time of 2 min was used. A fragment of β -actin was amplified as a control, using the following primers 5'-ATGGATGACGATATCGCTGCGCTGG-3' and 5'-GGTCATCTTTTCACGGTTGGCCTTAGGGT-3' and thermal cycling was performed for 28 cycles with an annealing temperature of 65°C, and extension of 30 sec.

Western Blot Analysis of Tissue Expression and Regulation by WY-14,643 and Fasting- Tissue expression of PTE-Ia at protein level was examined in muscle, heart, lung, brown adipose tissue, brain, liver and kidney from Sv/129 male mice. The regulation of expression by WY-14,643 and fasting was investigated in wild-type and PPAR α -null mice. Tissue pieces (about 0.1 g in 200 μ l buffer) were homogenized in 50 mM potassium phosphate buffer, pH 7.0. Fifty micrograms of protein was analyzed by Western blot as described (14), using an anti-rabbit PTE-Ia antibody (Sigma Genosys) generated against the first 15 amino acids of the protein, resulting in an antibody that specifically recognizes the long variant of PTE-Ia (5':1).

RESULTS

cDNA Cloning and Sequence Analysis- We previously identified and cloned a novel gene family of four type-I acyl-CoA thioesterases, with members identified in cytosol (CTE-I), mitochondria (MTE-I) and peroxisomes (PTE-Ia and PTE-Ib) (17). These genes are localized in a cluster on chromosome 12 in mouse. Recent EST database searches have identified two further putative peroxisomal Type-I acyl-CoA thioesterases, namely PTE-Ic and PTE-Id, which are also located in the same cluster on mouse chromosome 12 (Fig. 1). Of the four putative peroxisomal genes identified in mouse, PTE-Ia and PTE-Ic show highest homology to each other, and were therefore cloned and characterized

together in this study. The genomic organization for PTE-Ia and PTE-Ic were obtained from the mouse genomic database (ENSEMBL, www.ensembl.org), as outlined in Fig. 2A. Both proteins are encoded by 3 exons, spaced by 2 introns. Analysis of EST sequences for PTE-Ia suggested the possible existence of an additional small exon (30-37 bp) further upstream in the 5'-end, which results in two different splice variants depicted as 5':1 and 5':2 in Fig. 2A. The existence of these two splice variants was further supported by sequence analysis, since the exon-intron boundaries are consistent with the donor-acceptor splice rules, as shown in Fig. 2B. Furthermore, these two splice variants were amplified by RT-PCR from liver and kidney (see below).

Based on the genomic sequences, the corresponding ORFs were amplified by RT-PCR and fully sequenced. The full-length cDNAs were assembled based on ESTs corresponding to the 5' and 3' untranslated regions (UTRs) and verified by analysis of mouse genomic sequences. Sequence analysis of the gene products for PTE-Ia and PTE-Ic show a sequence identity of 82% at amino acid level in their open reading frames (Fig. 3). The cDNAs isolated for PTE-Ia and PTE-Ic encode proteins of 432 and 421 amino acids, with calculated molecular masses of 47.4 kDa and 46.6 kDa respectively. Interestingly, the PTE-Ia cDNA of the PTE-Ia 5':1 splice variant contains an extra 11 amino acids in the amino-terminal end, while the 5':2 splice variant splices out the first methionine, with the protein starting at the second methionine, similar to the cytosolic and the other peroxisomal thioesterases (17). Both sequences end –AKL at their carboxy-terminal, which is a variant of the peroxisomal consensus type 1 targeting signal of –SKL (PTS1) (25). A catalytic triad containing serine (S), histidine (H), and aspartic acid (D) residues, located at positions 232, 358 and 324 of PTE-Ic, has been identified in this family of acyl-CoA thioesterases and is conserved also in these two enzymes (26).

PTE-Ia and PTE-Ic are Localized in Peroxisomes- The nomenclature of PTE-Ia and PTE-Ic were based on their putative consensus PTS1 of –AKL at their carboxy-terminal ends. To test if these proteins are indeed peroxisomal, we cloned both PTE-Ia and PTE-Ic in-frame with GFP, which leaves the carboxy-terminal –AKL accessible. We transfected these plasmids into both control fibroblasts and fibroblasts from a Zellweger patient, which are unable to import

peroxisomal matrix proteins. Using immunofluorescence microscopy and a Tritc-labeled secondary antibody to GFP, PTE-Ia showed a punctate pattern of expression in control fibroblasts, indicative of a peroxisomal localization (Fig. 4A). However, in Zellweger fibroblasts, transfection of PTE-Ia resulted in a diffuse GFP expression showing that PTE-Ia remained in the cytosol (Fig. 4B). PTE-Ic also showed a punctate pattern of expression in control fibroblasts, although some cytosolic staining was visible in this case (Fig. 4C). Again, in Zellweger fibroblasts, transfection of PTE-Ic resulted in a diffuse GFP expression (Fig. 4D). Due to the 11 amino acid extension in the amino-terminal of PTE-Ia (5':1), we also examined the possibility of a mitochondrial targeting of PTE-Ia. This was examined by expressing both the long (5':1) and the short (5':2) amino-terminal variants of PTE-Ia as carboxy-terminal GFP fusion proteins in fibroblasts. However the GFP experiments for these variants showed only cytosolic labeling with no mitochondrial localization (data not shown).

Recombinant Expression and Characterization- The cloning of the ORFs encoding PTE-Ia (5':1) and PTE-Ic into the *Nde I* site in the pET16b vector results in expression of the proteins as His-tagged fusion proteins, which allows for purification using affinity chromatography. Following purification on a Hi-Trap[®] column, the purified proteins were detected as single bands of about 47 kDa on SDS-PAGE stained with Coomassie Brilliant blue (data not shown). Following initial enzyme activity characterization of the recombinant protein, it was evident that PTE-Ia activity, but not PTE-Ic activity, was inhibited with substrates ranging from C₁₄-C₂₀ at concentrations higher than 5-10 μ M. However, addition of BSA to the reaction at an albumin/acyl-CoA ratio of 1:4.5 prevented inhibition (data not shown). Recombinant PTE-Ia and PTE-Ic were analyzed for acyl-CoA thioesterase activity, which was determined at several concentrations for a variety of acyl-CoA substrates, including saturated and unsaturated straight-chain acyl-CoAs, branched-chain acyl-CoAs and bile acid CoA-esters. Interestingly, in spite of the very high sequence homology, PTE-Ia and PTE-Ic showed different chain-length specificities for straight-chain acyl-CoAs. While PTE-Ia is a long-chain acyl-CoA thioesterase (highest activity with palmitoyl-CoA, C₁₆-CoA), PTE-Ic is a medium-chain thioesterase (highest activity with decanoyl-CoA, C₁₀-CoA)

(Fig. 5). Neither of the enzymes was active on bile acid-CoA esters (tested with choloyl-CoA and chenodeoxycholoyl-CoA). V_{max} and K_m values were calculated for those acyl-CoAs that were substrates for PTE-Ia and PTE-Ic (Table I). Further support for the difference in acyl-CoA chain-length specificity stems from differences in the K_m values. The K_m values for PTE-Ia were generally much lower for long-chain acyl-CoAs than those for PTE-Ic. Also 4,8-dimethylnonanoyl-CoA (DMN-CoA), a metabolite in the β -oxidation of pristanic acid, was found to be a better substrate for PTE-Ic than for PTE-Ia (Table I).

We previously showed that mouse PTE-2, a peroxisomal acyl-CoA thioesterase which hydrolyzes a variety of CoA esters, is strongly inhibited by free CoASH ($IC_{50} \approx 10-15 \mu M$) (19), suggesting that PTE-2 regulates intraperoxisomal levels of free CoASH. We therefore tested the effect of CoASH on the acyl-CoA thioesterase activity of PTE-Ia and PTE-Ic. However, neither PTE-Ia nor PTE-Ic were markedly inhibited by CoASH when tested at concentrations up to 500 μM , (data not shown), suggesting that PTE-Ia and PTE-Ic are not involved in regulation of intra-peroxisomal CoASH levels, but rather regulate intra-peroxisomal acyl-CoA levels.

Tissue Expression- The tissue expression of PTE-Ia and PTE-Ic at mRNA level was examined using RT-PCR in several tissues, with β -actin as a control (Fig. 6A). PTE-Ia and PTE-Ic showed a selective tissue expression, with PTE-Ia (both splice variants 5':1 and 5':2 amplified in the same PCR product) highly expressed in kidney and only weakly expressed in the other tissues examined. PTE-Ic is highly expressed in spleen, brain, testis and proximal and distal intestine, and weakly expressed in the other tissues. Both PTE-Ia and PTE-Ic are weakly expressed in liver from untreated mice, but strongly increased at mRNA level by treatment of mice with WY-14,643 (Fig. 6A). A splice variant of PTE-Ic identified as the lower band on the gel in Fig. 6A (marked with an asterisk) was induced in liver by treatment with WY-14,643. Western blot analysis for PTE-Ia (5':1) on muscle, heart, lung, brown adipose tissue, brain, liver and kidney showed no detectable protein expression in these tissues, except for liver, with an induction seen in WY-14,643 treated liver. In kidney, no immunoreactive protein was seen (Fig. 6B), but was detectable in fasted kidney (where PTE-Ia 5':1 may be strongly upregulated). As mentioned

above, in one of the splice variants for PTE-Ia (5':2), the nucleotides encoding the first methionine is spliced out, producing a protein that is 11 amino acid shorter and which lacks the epitope recognized by the PTE-Ia antibody. Therefore the antibody recognizes only the PTE-Ia 5:1 splice variant. The lack of immunoreactive protein in muscle, heart, lung, brown adipose tissue, brain, and control kidney thus suggested that the PTE-Ia 5':1 splice variant is expressed only in liver, and that the high expression in kidney by RT-PCR (Fig. 6A) represents the 5':2 splice variant. To test this possibility, we PCR-amplified the two splice variants in liver and kidney. As shown in Fig. 6C, the PTE-Ia 5':2 splice variant is expressed in kidney, but not in liver. In contrast, the PTE-Ia 5':1 splice variant encoding the longer PTE-Ia protein containing the antibody epitope could be PCR-amplified from liver, and this mRNA was increased in response to WY-14,643 treatment (data not shown).

Regulation of PTE-Ia and PTE-Ic Expression by WY-14,643 Treatment and Fasting- RT-PCR was carried out on total RNA from untreated and WY-14,643 treated liver from wild-type (+/+) and PPAR α -null (-/-) mice. Both PTE-Ia (splice variants 5':1 and 5':2) and PTE-Ic were highly induced by WY-14,643 treatment in wild-type mice, but were not induced in the PPAR α -null animals, showing that this induction is mediated via PPAR α (Fig. 7A, upper panel). This induction was confirmed also at protein level by Western blot analysis for PTE-Ia (Fig. 7A, lower panel) and by Northern blot analysis for both PTE-Ia and PTE-Ic (data not shown). Northern blot analysis identified two mRNA transcripts of approximately 2.2 kb and 2.8 kb for PTE-Ia, which probably account for the difference in size of the two cDNA sequences for the 5':1 and 5':2 transcripts (approx. 750 bp). Regulation of both PTE-Ia and PTE-Ic mRNA was also examined in liver, kidney and heart from mice fasted for 24 hours. RT-PCR showed that PTE-Ia was up-regulated by fasting in mouse liver in wild-type animals, but not in the PPAR α -null mice (Fig. 7B, upper panel). This PPAR α -dependent up-regulation by fasting was also confirmed at protein level by Western blot analysis for PTE-Ia (Fig. 7B, lower panel).

As PTE-Ia (both splice variants 5':1 and 5':2) showed a very high expression in kidney, we examined the regulation of the PTE-Ia in this organ during the physiological condition of fasting. PTE-Ia mRNA expression was upregulated

by fasting in mouse kidney in wild-type animals, and again this up-regulation was abolished in the PPAR α -null mice (Fig. 8). In contrast, expression of PTE-Ic showed no regulation by fasting either in liver or kidney (Fig. 7B, upper panel, Fig. 8), and neither PTE-Ia nor PTE-Ic was regulated by fasting in heart (data not shown).

DISCUSSION

From previous work using molecular cloning and database mining, we have now identified six highly homologous acyl-CoA thioesterase genes that are located in a cluster on mouse chromosome 12, of which four genes encode putative peroxisomal enzymes. These enzymes show approximately 40% sequence identity to the bile acid-CoA:amino acid *N*-acyltransferase (BACAT) (26), an enzyme involved in the conjugation of bile acids to glycine or taurine (27-29). In addition, we have identified two further genes that are apparently located close to the gene for BACAT on mouse chromosome 4. These two genes also encode putative peroxisomal acyl-CoA thioesterases. This raised the question as to why there are so many peroxisomal acyl-CoA thioesterases in mouse. To address this issue, we have now cloned and characterized two of these genes that we named PTE-Ia and PTE-Ic, and show that they are indeed peroxisomal enzymes with different functions based on their different acyl-CoA chain-length specificities and tissue expression. Elucidation of the organization of the PTE-Ic gene shows that the open reading frame is encoded by three exons, similar to the PTE-Ia and other Type-I genes (17). In this gene family identified, the cytosolic (CTE-I) and the mitochondrial (MTE-I) thioesterases show the highest degree of sequence identity to each other (>90%), while the PTE-Ia and PTE-Ic are the most similar peroxisomal thioesterases with a sequence identity of 82%. Most of the sequence differences between all six thioesterases are found in the third exon, in the area where the active-site catalytic triad is located, which indicates that these thioesterases have different substrate specificities. Sequence analysis of PTE-Ia and PTE-Ic shows that there are two regions within the third exon that are less conserved, amino acids 257-280 of PTE-Ic (29% sequence identity) and amino acids 369-384 (22% sequence identity). The enzyme activity measurements showed that indeed these two enzymes have different

substrate specificities, with PTE-Ia acting as a long-chain acyl-CoA thioesterase, and PTE-Ic as a medium-chain acyl-CoA thioesterase.

Examination of tissue expression at mRNA level showed that these enzymes have a different and very selective tissue expression, with PTE-Ia being highly expressed in kidney and a lower expression in the rest of the tissues examined, while PTE-Ic is highly expressed in spleen, brain, testis, proximal and distal intestine and showed lower expression in the rest of the tissues. The expression of both of these enzymes is highly up-regulated in liver by the hypolipidemic drug WY-14,643 at both mRNA and protein level, and this effect is mediated via PPAR α . Although the highest PTE-Ia mRNA level was found in kidney, surprisingly, there was no detectable protein in kidney from untreated animals (Fig. 6B). In contrast, protein was readily detected in liver, although the mRNA levels were much lower in liver than in kidney (Fig. 6A). EST database searches suggested that the 5'-untranslated region of PTE-Ia may be differently spliced, with one of the variants apparently splicing out the first start methionine, resulting in a truncated protein lacking the first 11 amino acids (5':2) (corresponding to most of the epitope against which the PTE-Ia antibody was raised). Two EST sequences were found for this splice variant 5':2 (Accession numbers AW044864 and AI788456), both being derived from mouse kidney. Our results now show that PTE-Ia 5':2 is expressed in kidney, but not in liver, while the longer PTE-Ia protein (containing the extra 11 amino acids) appears to be more liver specific, resulting in different tissue expression of these two proteins. As yet it is not known what regulates the splicing within the different tissues, but the liver specific expression of PTE-Ia (5':1) may be regulated by liver-specific transcription factors. The function of the 11 extra amino acids at the amino-terminal of PTE-Ia is not clear. Sequence analysis did not indicate the presence of an amino-terminal type-2 peroxisomal targeting signal (PTS-2) which is present in some peroxisomal matrix proteins (30), nor the presence of a mitochondrial targeting signal. This was verified experimentally by expression of both the 5':1 and 5':2 PTE-Ia splice variants as carboxy-terminal GFP fusion proteins in human skin fibroblasts. Both carboxy-terminal PTE-Ia/GFP fusion proteins localized to the cytosol. In mammalian genomes, it now appears that alternative splicing of many genes results in several

different gene products (31), which may have different functions or show a distinct tissue expression. Indeed, a splice variant for PTE-Ic was also detected (marked with an asterisk), which splices out 118 bp of the open reading frame, resulting in a premature stop codon, which should result in an inactive protein that does not contain the active site histidine and aspartic acid residues. The expression of this splice variant also shows tissue selectivity and regulation by WY-14,643 (Fig. 6A and Fig. 7A).

Putative Functions for PTE-Ia and PTE-Ic in Peroxisomes:

The selective tissue expression and variation in regulation indicates different functions for these two enzymes in peroxisomal lipid metabolism in different organs. Peroxisomes have important functions in the degradation of a broad spectrum of lipids, in particular lipids that are poorly metabolized by mitochondria (for reviews, see (2,32,33)). The main function of peroxisomal α -oxidation is the metabolism of various carboxylic acids, for example prostanoids and dicarboxylic fatty acids, into chain-shortened, more hydrophilic compounds that can be excreted in the urine as free carboxylic acids. Alternatively, peroxisomes chain-shorten long- and very long-chain acyl-CoAs, which may then be transported to mitochondria for further oxidation. The transport of fatty acids across the peroxisomal membrane is not fully understood, but based on studies in mammalian cells and yeast it appears that several mechanisms may operate in peroxisomes. Medium-chain fatty acids may be transported across the peroxisomal membrane as free acids, and become activated to the corresponding CoA-ester inside the peroxisome (34). In contrast, long-chain fatty acids, trihydroxycoprostanic acid and prostanoids become activated outside the peroxisome, followed by transport of the CoA-esters across the peroxisomal membrane (for reviews, see (35,36)). Since medium-chain fatty acids are transported into the peroxisome, it is feasible to assume that they can also be transported out of the peroxisome, for example in the case of chain-shortened fatty acids. It is hypothesized that PTE-Ia and PTE-Ic may be involved in this process by hydrolysis of long/medium-chain fatty acyl-CoA esters to the free fatty acid, for transport out of the peroxisome to the mitochondria or endoplasmic reticulum for further α - or β -oxidation. We also examined the activity of PTE-Ia and PTE-Ic towards the α -oxidation intermediate 3-OH palmitoyl-CoA, but

these enzymes had very low activity towards this compound, suggesting that they can hydrolyze either the substrate or product of the α -oxidation pathway in peroxisomes, but not intermediates in these pathways. The induction of both PTE-Ia and PTE-Ic by both peroxisome proliferators and/or fasting in liver and kidney is in line with an increase in α -oxidation activity in these organs during conditions that increase oxidation capacity.

It has been established that long/medium chain fatty acids are transported to mitochondria as the carnitine ester for complete α -oxidation. Peroxisomes contain a carnitine octanoyltransferase that can potentially convert medium-chain acyl-CoAs to the corresponding carnitine ester for transport to mitochondria. The physiological role of this carnitine octanoyltransferase is not fully clear, but it was shown that this enzyme converts 4,8-dimethylnonanoyl-CoA, a metabolite of pristanic acid, to its corresponding carnitine ester, which is required for its transport to mitochondria for further α -oxidation (37). In contrast, essentially no information is available concerning transport of free CoASH across the peroxisomal membrane. Two important functions can therefore be proposed for acyl-CoA thioesterases in peroxisomes (i) to terminate chain-shortening of various carboxylic acids to promote transport out of the peroxisome for transport to mitochondria for further oxidation (short-, medium- and long-chain fatty acids), or for secretion into urine (dicarboxylic fatty acids and chain-shortened prostanoids), and (ii) to regulate intra-peroxisomal levels of acyl-CoA/CoASH.

In mouse six different Type I acyl-CoA thioesterases have been identified, one cytosolic, one mitochondrial and four peroxisomal acyl-CoA thioesterases (PTE-Ia-d) ((17), this study and unpublished data). In addition, peroxisomes contain another structurally unrelated acyl-CoA thioesterase, called PTE-2. This enzyme was initially identified as a HIV-1 Nef binding protein (21,22), and subsequently further characterized as an acyl-CoA thioesterase in mouse, human, yeast and rat (19,20,23,38). Characterization of PTE-2 in mouse showed it to be the major acyl-CoA thioesterase in peroxisomes, hydrolyzing a broad range of acyl-CoA esters. The activity of recombinant PTE-2 is strongly regulated by CoASH ($IC_{50} \approx 10 \mu M$), suggesting that PTE-2 regulates intra-peroxisomal CoA-levels (19). Comparison of the acyl-CoA thioesterase

activity in isolated peroxisomes with recombinant PTE-2 suggests that this enzyme is responsible for essentially all thioesterase activity except for the activity on medium- to long-chain acyl-CoAs which is induced in rat liver peroxisomes by peroxisome proliferator treatment (16). The findings reported in this study that PTE-Ia and PTE-Ic are peroxisome proliferator-induced long- and medium-chain acyl-CoA thioesterases therefore provides data to show that in principle PTE-2, PTE-Ia and PTE-Ic are responsible for the peroxisomal acyl-CoA thioesterase covering C₂-C₂₂ acyl-CoAs. It is therefore likely that the remaining uncharacterized peroxisomal acyl-CoA thioesterases have activities towards other more specific substrates. Experiments are presently underway in our laboratory to examine this.

Acknowledgements

This study is supported by the Swedish Research Council, Åke Wibergs stiftelse, Hjärt-Lungfonden, Svenska Sällskapet för Medicinsk Forskning, Lars Hiertas Minne, Fredrik och Ingrid Thuring's Stiftelse, Ruth och Richard Juhlin's Stiftelse, Stifelsen Professor Nanna Svartz fond and National Network for Cardiovascular Research (Sweden).

TABLE I***Calculated V_{max} and K_m values for recombinant PTE-Ia and PTE-Ic***

Acyl-CoA thioesterase activity for PTE-Ia and PTE-Ic was measured with different acyl-CoA substrates at various concentrations. V_{max} and K_m was calculated using Sigma Plot Enzyme Kinetics program. Activities were measured on three different recombinant protein preparations for PTE-Ia and on two different recombinant protein preparations for PTE-Ic. Results from one representative experiment are shown. DMN: dimethylnonanoyl-CoA. ND: not detectable.

Acyl-CoAs □	PTE-Ia		PTE-Ic	
	V_{max} ($\mu\text{mol}/\text{min}/\text{mg}$)	K_m (μM)	V_{max} ($\mu\text{mol}/\text{min}/\text{mg}$)	K_m (μM)
Hexanoyl	0.02	10.9	0.23	28.4
Octanoyl	0.23	46.2	0.74	7.7
Decanoyl	0.87	7.7	1.20	18
Lauroyl	1.40	7.6	1.10	7.6
Myristoyl	1.60	3.8	0.83	5.6
Palmitoyl	1.85	4.0	0.49	15.9
Palmitoleoyl	0.93	2.8	0.32	7.0
Stearoyl	1.43	4.2	0.38	34.8
Oleoyl	0.85	4.6	0.14	8.9
Linoleoyl	0.63	2.6	0.17	32.5
Arachidoyl	0.71	2.2	0.18	32.7
Arachidonoyl	0.70	7.2	0.23	1.6
Behenoyl	0.37	2.3	ND□	ND
Lignoceroyl	0.20	6.3	ND□	ND
Cerotoyl	0.22	4.5	ND	ND□
DMN	0.32	16.9	0.81	32.3

Figure legends

Fig. 1. Genomic localization of PTE-Ia and PTE-Ic. The Type-I acyl-CoA thioesterase gene cluster consists of six genes encoding one mitochondrial acyl-CoA thioesterase (MTE-I), one cytosolic acyl-CoA thioesterase (CTE-I) and four putative peroxisomal acyl-CoA thioesterases (PTE-Ia/b/c/d), which are localized within 120-kb on chromosome 12 in mouse.

Fig. 2. Structural organization of the PTE-Ia and PTE-Ic genes. (A) The open reading frame for both PTE-Ia and PTE-Ic is encoded by three exons (boxes), spaced by two introns (broken lines). EST database searches identified two 5'-variants of the PTE-Ia, which are denoted 5':1 and 5':2, and contain a short exon encoding a further 5' untranslated region. The 5':1 splice variant contains the first in-frame ATG, encoding an 11 amino-acid longer PTE-Ia. In the 5':2 splice variant, the first ATG is spliced out, encoding a PTE-Ia protein which is 11 amino acids shorter. TGA: stop codon (B) Sequence alignment and comparison of the 5':1 and 5':2 splice variants. Nucleotides of the open reading frame are shown in capital letters, with the ATG codons underlined. Splice donor and acceptor sites are shown in italics. In 5':1, 547 bp are spliced out, and in 5':2 1293 bp are spliced out. In the sequence corresponding to 5':1, 719 bp (-719) were omitted to allow sequence comparison to 5':2.

Fig. 3. Sequence alignment of PTE-Ia and PTE-Ic. Alignment of the amino acid sequences of PTE-Ia and PTE-Ic was performed using the Clustal X method. PTE-Ia 5':1 commences at the first methionine, while 5':2 commences at the second methionine. Individual exon boundaries are indicated. The catalytic triad consisting of a serine (corresponding to serine 232 in the PTE-Ic), a histidine (358) and an aspartic acid (324) residue is indicated with arrowheads. Both enzymes contain a carboxy-terminal peroxisomal type 1 targeting signal of -AKL.

Fig. 4. PTE-Ia and PTE-Ic are peroxisomal proteins. Human skin fibroblasts were transfected with PTE-Ia/NT-GFP or PTE-Ic/NT-GFP and processed for immunofluorescence microscopy as outlined in Experimental Procedures. The

cellular localization of PTE-Ia and PTE-Ic was examined in control fibroblasts or Zellweger fibroblasts using a Tritc-labeled anti-GFP antibody: (A) PTE-Ia in control fibroblasts (B) PTE-Ia in Zellweger fibroblasts (C) PTE-Ic in control fibroblasts (D) PTE-Ic in Zellweger fibroblasts.

Fig. 5. Kinetic characterization of recombinant PTE-Ia and PTE-Ic. Recombinant PTE-Ia and PTE-Ic were expressed in *Escherichia coli* as His-tagged proteins and purified by affinity chromatography as described in Experimental Procedures. Acyl-CoA thioesterase activity was measured at 25 μ M substrate concentration, with the addition of bovine serum albumin at a molar ratio of 1:4.5 of BSA:acyl-CoA for C₁₄-C₂₀-CoAs in the case of PTE-Ia. The figure shows data from one representative experiment. The activity measurements were carried out on three different recombinant protein preparations for PTE-Ia and on two different recombinant protein preparations for PTE-Ic.

Fig. 6. Tissue expression of PTE-Ia and PTE-Ic. (A) The tissue expression of PTE-Ia (both 5':1 and 5':2 splice variants amplified) and PTE-Ic was examined using RT-PCR, with β -actin as a control. The PTE-Ic splice variant is indicated with an asterisk * (B) Western blot analysis was carried out on 50 μ g of protein from each tissue, using an anti-PTE-Ia antibody as described in Experimental Procedures. (C) RT-PCR from mouse liver and kidney using primers to amplify the PTE-Ia 5':2 variant. The negative control (NC) contained no RNA. MM: molecular marker.

Fig. 7. Regulation of PTE-Ia and PTE-Ic in mouse liver by WY-14,643 treatment and fasting. (A) Wild-type (+/+) or PPAR α -null (-/-) mice were treated with 0.1% WY-14,643 for one week. The mRNA levels of PTE-Ia (both 5':1 and 5':2 splice variants amplified) and PTE-Ic were examined in mouse liver using RT-PCR, with β -actin as a control (**upper panel**). The PTE-Ic splice variant is indicated with an asterisk *. Western blot analysis was carried out on 50 μ g liver protein from two wild-type (+/+) and PPAR α -null (-/-) mice treated with 0.1% WY-14,643 for one week, using an anti-PTE-Ia antibody as described in Experimental Procedures (**lower panel**). (B) Wild-type (+/+) or PPAR α -null (-/-) mice were fasted for 24 hours. The mRNA levels of PTE-Ia

(both 5':1 and 5':2 splice variants amplified) and PTE-Ic were examined in liver using RT-PCR, with β -actin as a control. In all cases, the negative control (NC) contained no RNA. MM, molecular marker (**upper panel**). Western blot analysis was carried out on 50 μ g of liver protein from two wild-type (+/+) and two PPAR α -null (-/-) mice fasted for 24 hours, using an anti-PTE-Ia antibody as described in Experimental Procedures (**lower panel**).

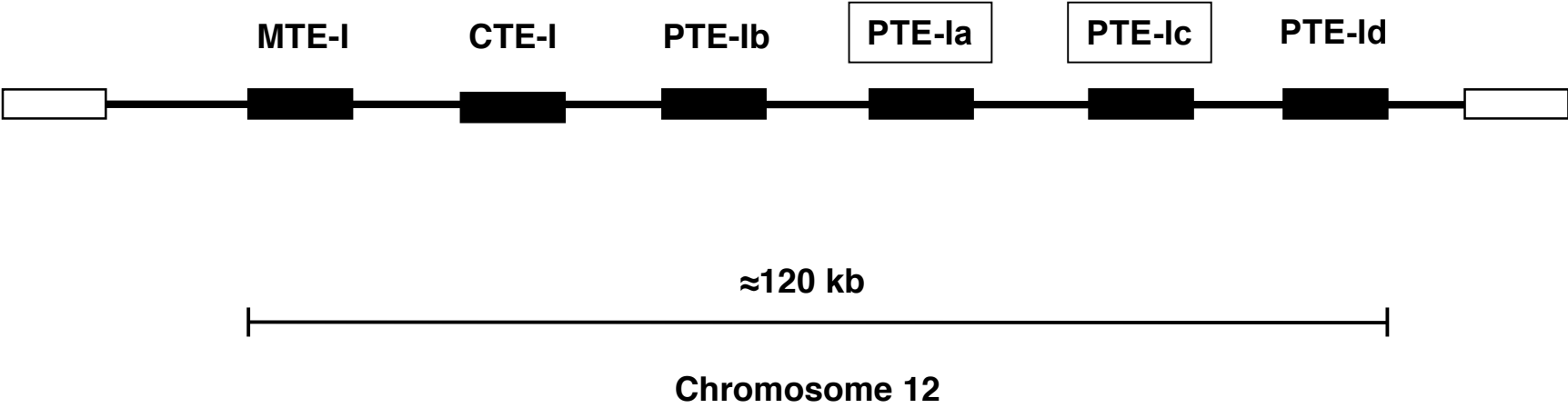
Fig. 8: Regulation of PTE-Ia and PTE-Ic by fasting in kidney. Wild-type (+/+) or PPAR α -null (-/-) mice were fasted for 24 hours. The mRNA levels of PTE-Ia and PTE-Ic were examined in kidney using RT-PCR, with β -actin as a control. The negative control (NC) contained no RNA. MM, molecular marker.

References

1. Reddy, J. K., and Mannaerts, G. P. (1994) *Annu. Rev. Nutr.* **14**, 343-370
2. Wanders, R. J. A., Vreken, P., Fedinandusse, S., Jansen, G. A., Waterham, H. R., van Roermund, C. W. T., and Van Grunsven, E. G. (2001) *Biochem. Soc. Trans.* **29**, 250-267
3. Diczfalusy, U., Kase, B. F., Alexson, S. E. H., and Björkhem, I. (1991) *J. Clin. Invest.* **88**, 978-984
4. Nemali, M. B., Usuda, N., Reddy, M. K., Oyasu, K., Hashimoto, T., Osumi, T., Rao, M. S., and Reddy, J. K. (1988) *Cancer Res.* **48**, 5316-5324
5. Issemann, I., and Green, S. (1990) *Nature* **347**, 645-650
6. Lee, S. S., Pineau, T., Drago, J., Lee, E. J., Owens, J. W., Kroetz, D. L., Fernandez-Salguero, P. M., Westphal, H., and Gonzalez, F. J. (1995) *Mol. Cell. Biol.* **15**, 3012-3022
7. Forman, B. M., Chen, J., and Evans, R. M. (1997) *Proc. Natl. Acad. Sci. U.S.A.* **94**, 4312-4317
8. Kliewer, S. A., Sundseth, S. S., Jones, S. A., Brown, P. J., Wisely, G. B., Koble, C. S., Devchand, P., Wahli, W., Willson, T. M., Lenhard, J. M., and Lehmann, J. M. (1997) *Proc. Natl. Acad. Sci. U.S.A.* **94**, 4318-4323
9. Göttlicher, M., Widmark, E., Li, Q., and Gustafsson, J.-Å. (1992) *Proc. Natl. Acad. Sci. U.S.A.* **89**, 4653-4657
10. Keller, H., Dreyer, C., A., M., Ozato, K., and Wahli, W. (1993) *Proc. Natl. Acad. Sci. U.S.A.* **90**, 2160-2164
11. Kroetz, D. L., Yook, P., Costet, P., Bianchi, P., and Pineau, Y. (1998) *J. Biol. Chem.* **273**, 31581-31589
12. Kersten, S., Seydoux, J., Peters, J. M., Gonzalez, F. J., Desvergne, B., and Wahli, W. (1999) *J. Clin. Invest.* **103**, 1489-1498
13. Leone, T. C., Weinheimer, C. J., Kelly, D. P. (1999) *Proc. Natl. Acad. Sci. U.S.A.* **96**, 7473-7478
14. Hunt, M. C., Lindquist, P. J. G., Peters, J. M., Gonzalez, F. J., Diczfalusy, U., and Alexson, S. E. H. (2000) *J. Lipid Res.* **41**, 814-823
15. Hunt, M. C., and Alexson, S. E. H. (2001) *Prog. Lipid Res.* **41**, 99-130
16. Wilcke, M., and Alexson, S. E. H. (1994) *Eur. J. Biochem.* **222**, 803-811
17. Hunt, M. C., Nousiainen, S. E. B., Huttunen, M. K., Orii, K., Svensson, L. T., and Alexson, S. E. H. (1999) *J. Biol. Chem.* **274**, 34317-34326
18. Jones, J. B., and Gould, S. J. (2000) *Biochem. Biophys. Res. Commun.* **275**, 233-240
19. Hunt, M. C., Solaas, K., Kase, B. F., and Alexson, S. E. H. (2002) *J. Biol. Chem.* **277**, 1128-1138
20. Jones, J. M., Nau, K., Geraghty, M. T., Erdmann, R., and Gould, S. J. (1999) *J. Biol. Chem.* **274**, 9216-9223
21. Watanabe, H., Shiratori, T., Shoji, H., Miyatake, S., Okazaki, Y., Ikuta, K., Sato, T., and Saito, T. (1997) *Biochem. Biophys. Res. Commun.* **238**, 234-239
22. Liu, L. X., Margottin, F., Le Gall, S., Schwartz, O., Selig, L., Benarous, R., and Benichou, S. (1997) *J. Biol. Chem.* **272**, 13779-13785
23. Tilton, G. B., Shockey, J. M., and Browse, J. (2003) *J. Biol. Chem.* **279**, 7487-7494
24. Bradford, M. M. (1976) *Anal. Biochem.* **72**, 248-254

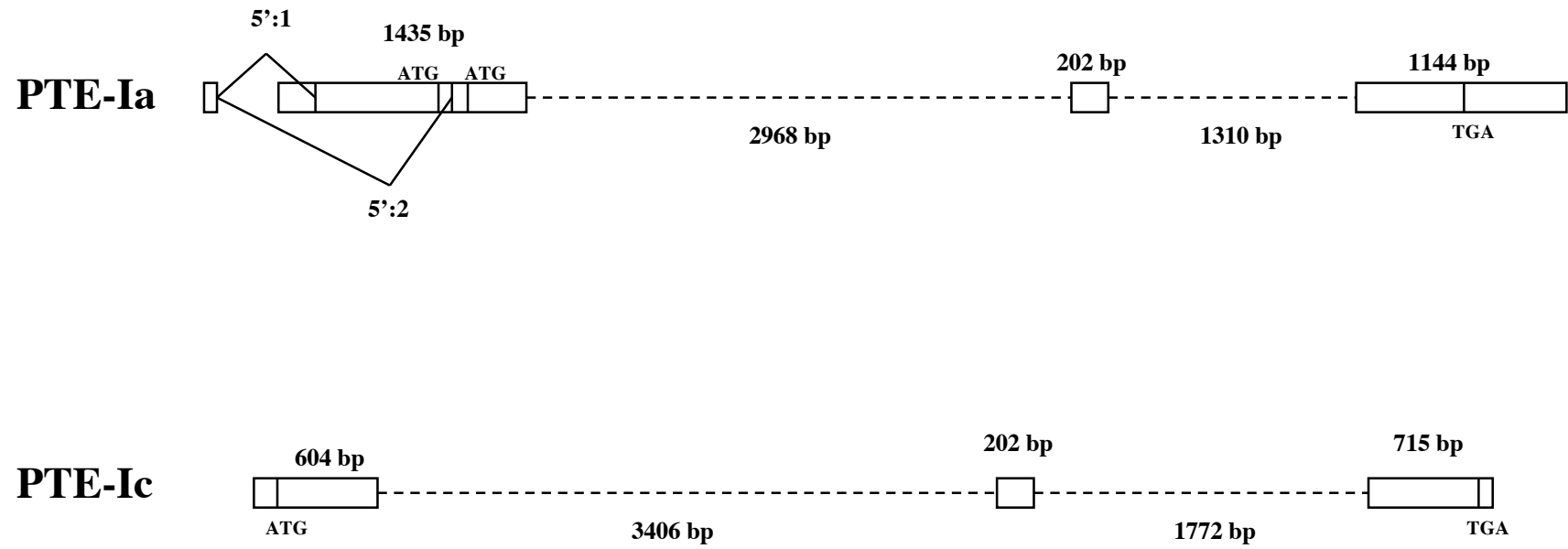
25. Gould, S. J., Keller, G. A., Hosken, N., Wilkinson, J., and Subramani, S. (1989) *J. Cell. Biol.* **108**, 1657-1664
26. Huhtinen, K., O'Byrne, J., Lindquist, P. J. G., Contreras, J. A., and Alexson, S. E. H. (2002) *J. Biol. Chem.* **277**, 3424-3432
27. Falany, C. N., Fortinberry, H., Leiter, E. H., and Barnes, S. (1997) *J. Lipid Res.* **38**, 1139-1148
28. Falany, C. N., Johnson, M. R., Barnes, S., and Diasio, R. B. (1994) *J. Biol. Chem.* **269**, 19375-19379
29. Furutani, M., Aarii, S., Higashitsuji, H., Mise, M., Fukumoto, M., Takano, S., Nakayama, H., Imamura, M., and Fujita, J. (1995) *Biochem. J.* **311**, 203-208
30. Legakis, J. E., and Terlecky, S. R. (2001) *Traffic* **2**, 252-260
31. Garcia-Blanco, M. A. (2003) *J. Clin. Invest.* **112**, 474-480
32. Van Veldhoven, P. P., and Mannaerts, G. P. (1999) *Adv. Exp. Med. Biol.* **466**, 261-272
33. Hiltunen, J. K., and Yong-Mei, Q. (2000) *Biochim. Biophys. Acta* **1484**, 117-128
34. van Roermund, C. W. T., Tabak, H. F., van Den Berg, M., Wanders, R. J. A., and Hetteema, E. H. (2000) *J. Cell Biol.* **150**, 489-498
35. Hetteema, E. H., Distel, B., and Tabak, H. F. (1999) *Biochim. Biophys. Acta* **1451**, 17-34
36. van Roermund, C. W. T., Waterham, H. R., Ijlst, L., and Wanders, R. J. A. (2003) *Cell. Mol. Life Sci.* **60**, 1838-1851
37. Ferdinandusse, S., Mulders, J., IJlst, L., Denis, S., Dacremont, G., Waterham, H. R., and Wanders, R. J. A. (1999) *Biochem. Biophys. Res. Commun.* **263**, 213-218
38. Ofman, R., el Mrabet, L., Dacremont, G., Spijker, D., and Wanders, R. J. A. (2002) *Biochem. Biophys. Res. Comm.* **290**, 629-634

Westin et al
Fig. 1.



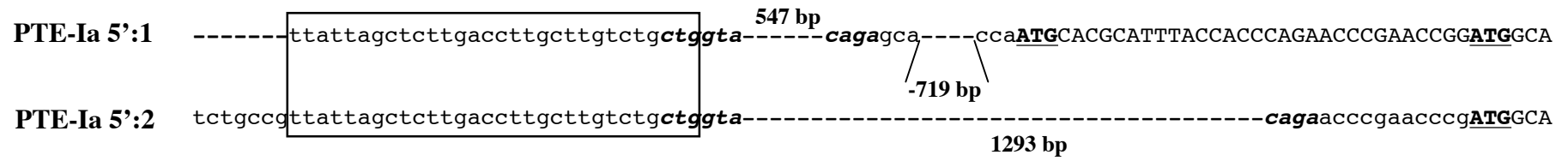
Westin et al
Fig. 2

A

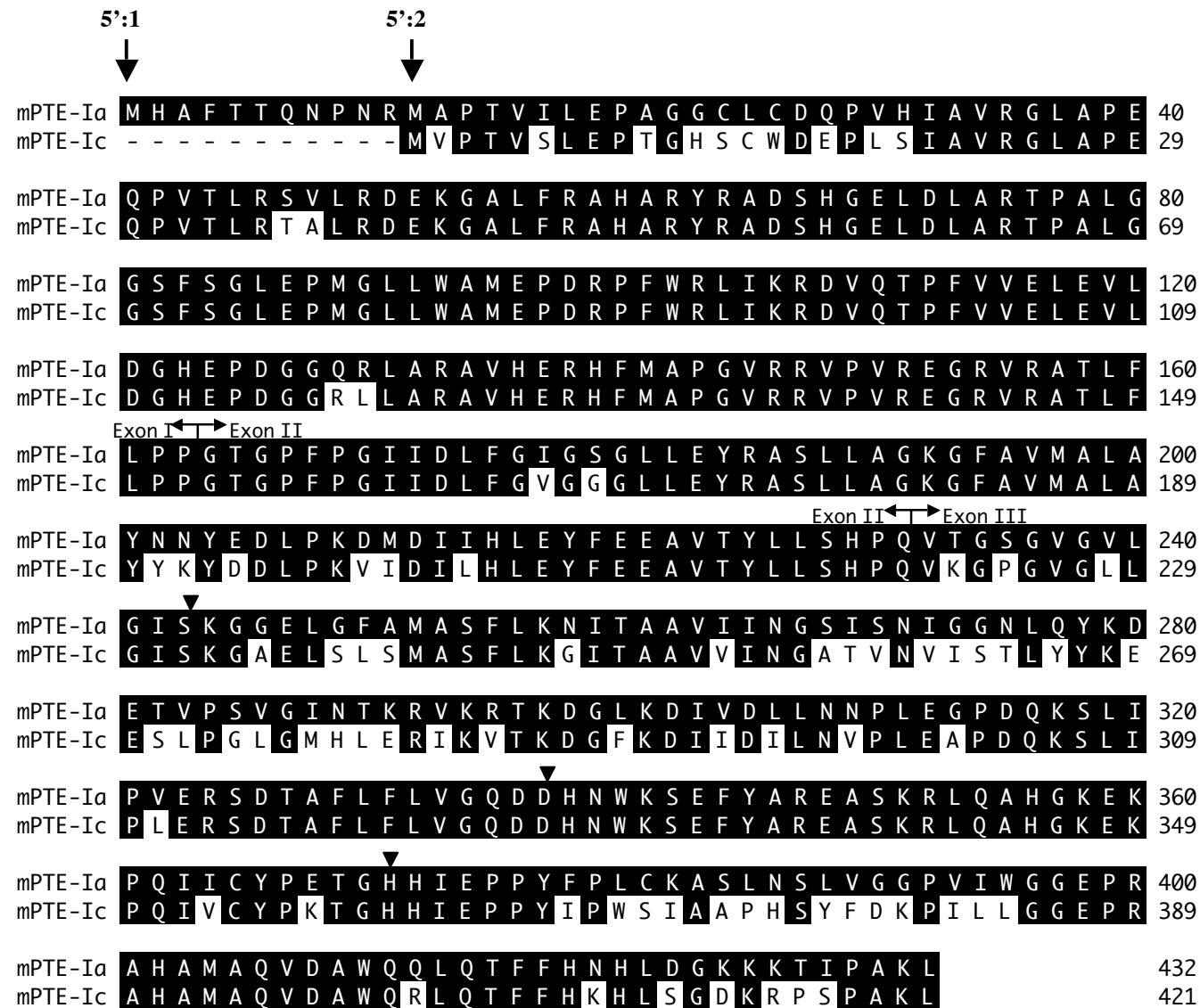


Westin et al
Fig. 2

B

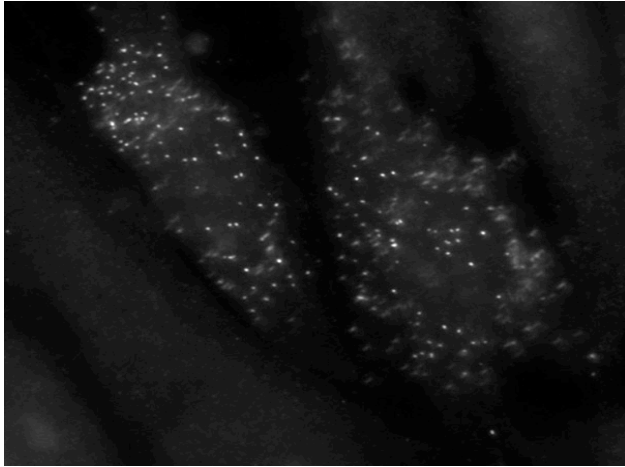


Westin et al
 Fig. 3.

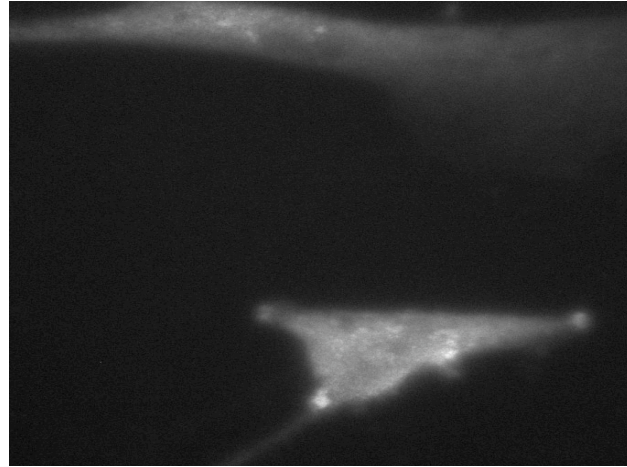


Westin et al
Fig. 4.

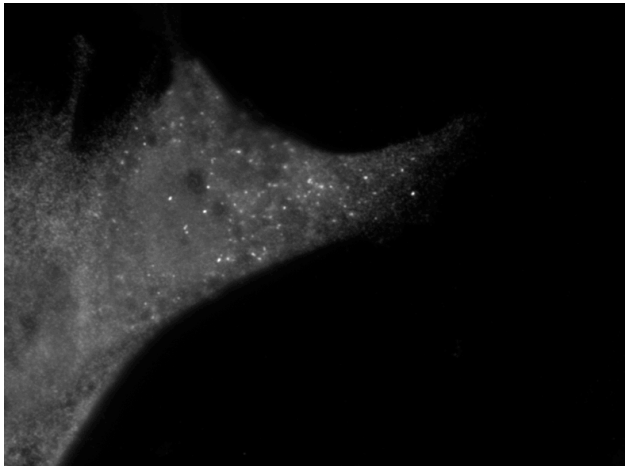
A



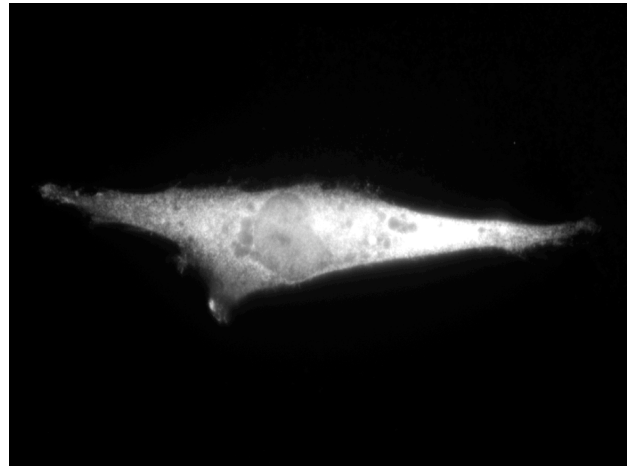
B



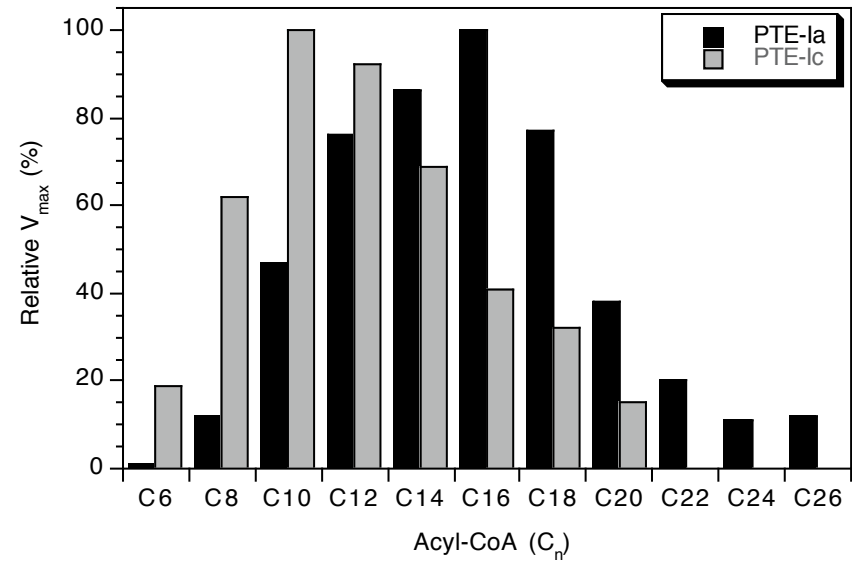
C



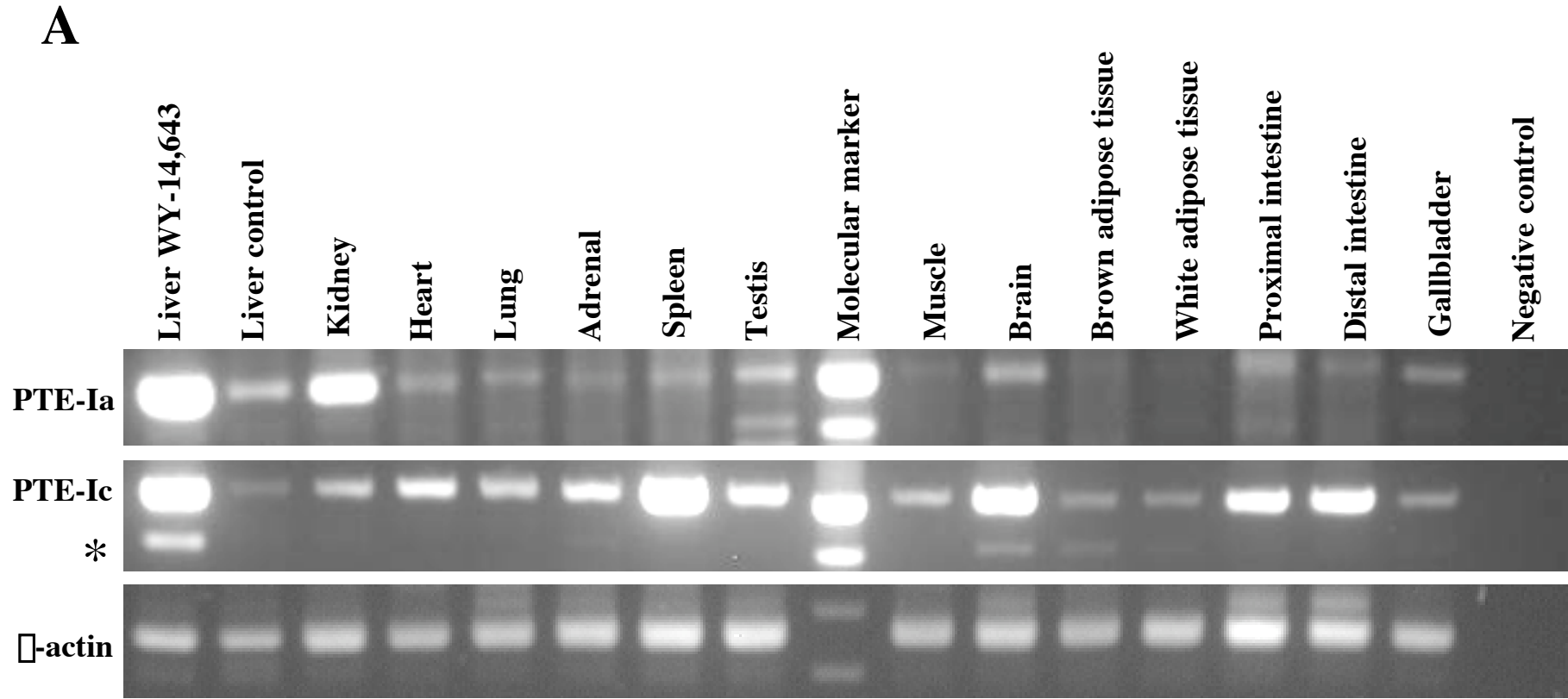
D



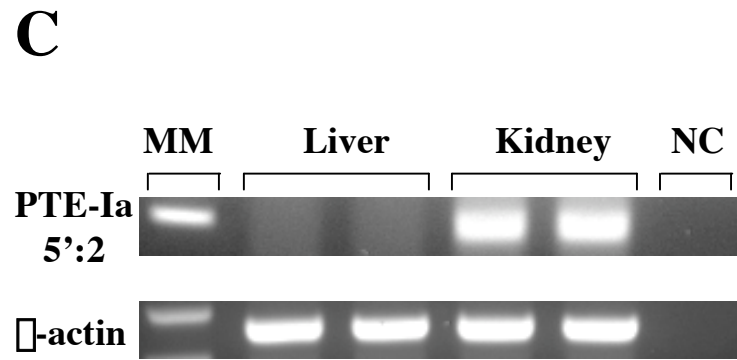
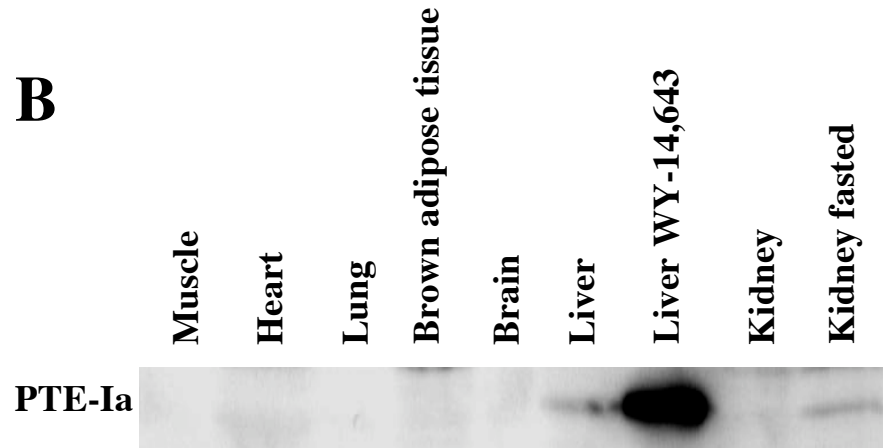
Westin et al
Fig. 5.



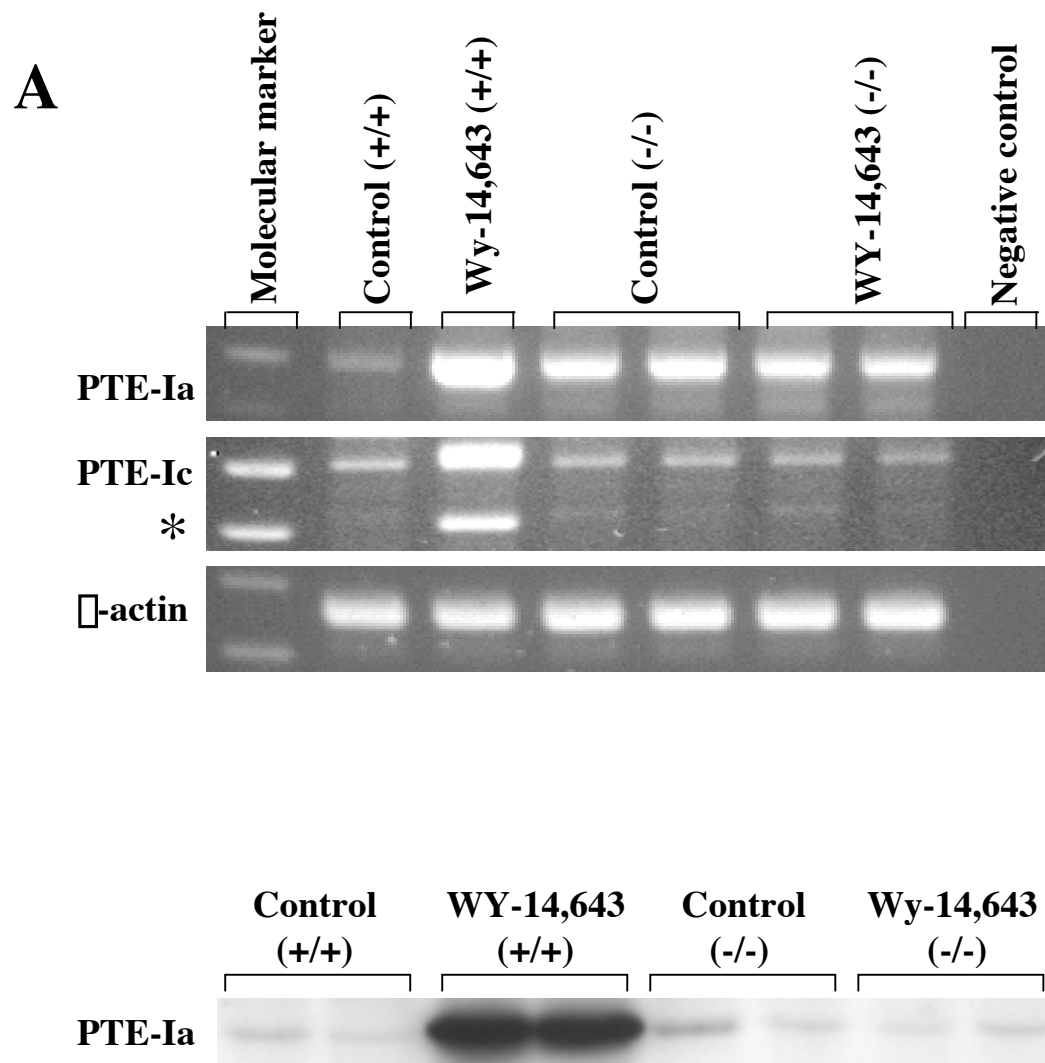
Westin et al
Fig. 6.



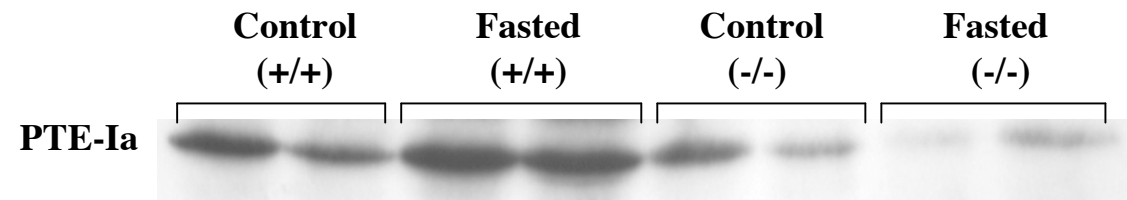
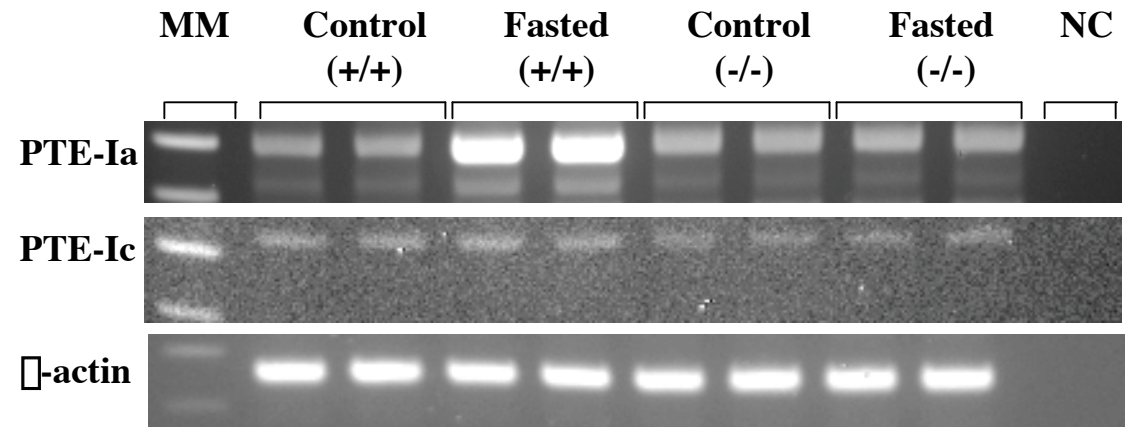
Westin et al
Fig. 6.



Westin et al
Fig. 7.



B



Westin et al
Fig. 8.

